Effect of soil moisture on canopy conductance of Amazonian rainforest

Philip P. Harris [a,*], Chris Huntingford [a], Peter M. Cox [b],
John H.C. Gash [a], Yadvinder Malhi [c]

[a] Centre for Ecology and Hydrology, Wallingford OX10 8BB, UK
[b] Hadley Centre, Meteorological Office, Bracknell RG12 2SY, UK
[c] Ecology and Resource Management, School of GeoSciences, University of Edinburgh, Edinburgh EH9 3JU, UK

Abstract

Estimates of canopy conductance, g_c, were derived from hourly eddy-covariance measurements of evaporation for a primary forest site near Manaus, Brazil, using an inverted Penman–Monteith equation. These data were used to calibrate Jarvis-type models of canopy conductance including and excluding a soil moisture dependence. A period of low canopy conductance in the observations coincided with low soil moisture and high humidity deficit. The model was able to capture this decrease in diurnal maximum g_c only when a soil moisture dependence was included. The optimised value of wilting point in the soil moisture function was $465\,\mathrm{m^3\,m^{-3}}$, which was comparable with estimates from soil hydraulic properties.
© 2003 Elsevier B.V. All rights reserved.

Keywords: Amazonia; Soil moisture; Conductance; Evaporation

1. Introduction

The Amazon basin is a centre of tropical heating and convection that contributes substantially to the general circulation of the atmosphere (Hastenrath, 1997; Costa and Foley, 1999). For this reason there has been particular interest in assessing the impact on climate of changes in Amazonian land cover, especially large-scale deforestation (Nobre et al., 1991; Gash et al., 1996; Hahmann and Dickinson, 1997). Results from global circulation model (GCM) simulations of climate following deforestation vary in their details, but there is a qualitative consensus that such loss

of rainforest would lead to reduced evaporation and increased temperatures in Amazonia (Stocker et al., 2001). More recent model simulations have shown that vegetated land cover in Amazonia has the potential to change in response to anthropogenically induced climate change (White et al., 1999; Cox et al., 2000). In these studies, climate change led to rainforest in Amazonia becoming an unsustainable ecosystem, which would be superseded by a mixture of shrubs, grassland and bare soil.

The land–atmosphere boundaries in most GCMs are described by soil-vegetation-atmosphere transfer (SVAT) schemes that calculate fluxes of heat, moisture and momentum from climate and soil moisture conditions. Central to SVATs are descriptions of stomatal conductance, which are often calibrated using observed water vapour fluxes from field sites. For

* Corresponding author. Tel.: +44-1491-692206;
fax: +44-1491-692338.
E-mail address: ppha@ceh.ac.uk (P.P. Harris).

example, Wright et al. (1996b) calibrated such models against flux data from Amazonian rainforest and deforested sites for use in deforestation GCM experiments.

Until now, many SVATs calibrated off-line for Amazonian rainforest have omitted a soil moisture dependence of canopy conductance. This was done under the assumption that either root depths are sufficient for the forest to maintain transpiration through the dry season or that significant soil moisture deficits are not observed (e.g. Wright et al., 1996a; Ashby, 1999). However, if these same models are used under conditions of low soil moisture, due to reduced rainfall in the future, then the response of the calibrated SVAT may not represent the true hydrological land-surface response.

Nepstad et al. (1994) found that forests in some parts of Amazonia required access to water to depths of at least 8 m in order to maintain transpiration through particularly dry periods. Sommer et al. (2002) suggest that because of this, soil water availability should be used more often in SVAT modelling studies. Malhi et al. (1998) observed a significant seasonality in maximum daytime photosynthesis that correlated with soil moisture content for a rainforest site near Manaus, Amazonas. Using a SVAT model, Williams et al. (1998) attributed this relationship to an increase in soil–root hydraulic resistance during the dry season. Contrary to the perception that the rainforest is never water stressed, such studies suggest that vegetation in this region does respond to seasonal changes in soil moisture. Because of correlations between soil moisture, humidity deficit and air temperature, it is sometimes difficult to separate the effects of near-surface meteorology and soil moisture on canopy conductance without use of a model.

The aim of this study was to show whether or not changes in soil moisture supply affected the canopy conductance of rainforest. The detailed objectives were to estimate rainforest canopy conductance from eddy-covariance measurements of evaporation using an inverted Penman–Monteith (PM) equation for evapotranspiration, and to use a simple, parameter scarce model to highlight the influence of seasonal soil moisture change on canopy conductance over other meteorological factors. A Jarvis-type model of canopy conductance, based on Jarvis (1976) and extended by Stewart (1988), was applied including and

excluding a soil moisture dependence, and the results compared with previous studies for Amazon rainforest. It was not an objective of this study to produce a parameterisation of canopy conductance for use in GCM studies.

2. Description of site and data

The data used in this study are described in detail by Malhi et al. (1998, 2002), and only a summary is presented here. Field measurements were made at a site of primary tropical rainforest in the Reserva Biológica do Cuieiras ($2°35'$S, $60°06'$W), a forest reserve belonging to Instituto Nacional de Pesquisas da Amazônia, located roughly 60 km north of Manaus, Amazonas, Brazil. The meteorological data were collected from a 41.5 m tower situated on a broad lowland plateau (90 m above sea level), with the forest canopy at a height of approximately 30 m above the plateau. Water vapour fluxes were measured using an eddy-covariance system mounted at 46.5 m. The forest on the plateau is terra firme, so there is no seasonal flooding or surface water, and vegetation consists of mostly broad-leaved hardwoods and palms in the understorey (Williams et al., 1998). Above ground biomass is 300–350 t ha^{-1}, and leaf area index estimates for nearby sites range from 5.7 to 6.6 (Roberts et al., 1996).

The data set covered a 6-month period from 17 October 1995 to 8 May 1996, during which time most surface climate variables were available for all hours. Short periods of rainfall data were missing and these were filled with data from a nearby forest site. Whilst not ideal considering the convective nature of most rainfall in this region, rainfall data were used only to exclude from the analysis days when wet-canopy evaporation was likely to dominate transpiration. The absolute hourly rainfall amounts were not used in this study. For the 6-month period eddy-covariance moisture flux data were available for 53% of the time. A total of 2331 h of surface evaporation and weather station data were available for the analysis covering a period of 250 days from 17 October 1995 to 8 May 1996. Energy closure for this data set was 94%, higher than the values of 70–80% typically reported for eddy-covariance measurements at Amazonian rainforest sites (Malhi et al., 2002). This data set was chosen over others that included the dry season months

of July to October because the superior energy closure gave greater confidence in the estimates of canopy conductance calculated using observed fluxes of sensible and latent heat.

The climate at this site is characterised by little seasonal variation in temperature and a moderate seasonal variation in rainfall. The short dry season from July to October occurs when the intertropical convergence zone (ITCZ) is in the Northern Hemisphere. For the period of 1 September 1995 to 8 May 1996 the total rainfall was 1118 mm. September–April rainfall for Manaus city between 1901 and 1987 ranged from 852 to 2230 mm with a mean of 1650 mm. The mean temperature through the study period was 25.1 °C, with monthly means ranging from 24.2 °C in February to 26.9 °C in September.

The soils at this site are a yellow clay latosol (Brazilian classification) or oxisol (US classification), with clay and sand content of 80 and 10%, respectively. The available water capacity is calculated to be only about 70 mm m^{-1} in the upper metre (Correa, 1984) and about 30 mm m^{-1} below 2 m (Hodnett et al., 1996). Hodnett et al. estimate that the maximum water uptake below 2 m by vegetation can reach 250 mm in a dry year. Soil moisture data were available at roughly weekly intervals over the top 3.8 m.

3. Methods

SVAT schemes used in GCMs partition the available energy between fluxes of latent and sensible heat. The PM equation (Monteith, 1981) allows this calculation to be done without knowledge of surface temperature, which is not often measured. In the PM equation, biophysical control over transpiration is expressed for the canopy as a whole through canopy conductance, g_c (m s^{-1}), which is a function of near-surface meteorology. To obtain estimates of observed g_c, against which parameters in conductance models may be calibrated, the PM equation is rearranged to yield g_c^{obs} as a function of latent heat flux and near-surface meteorology thus,

$$g_c^{obs} = g_a \left[\frac{(\Delta A + \rho c_p D_1 g_a)}{\gamma \lambda E} - \frac{\Delta}{\gamma} - 1.0 \right]^{-1}. \quad (1)$$

Here g_c^{obs} is the observed canopy (or bulk stomatal) conductance for water vapour, λ the latent

heat of vapourisation (J kg^{-1}), E the moisture flux (kg m^{-2} s^{-1}), Δ the rate of change of saturated specific humidity with temperature (K^{-1}), A the available energy (W m^{-2}), ρ the density of dry air (kg m^{-3}), c_p the specific heat capacity of dry air (J kg^{-1} K^{-1}), g_a the aerodynamic conductance for water vapour (m s^{-1}) and γ the psychrometric constant (Pa K^{-1}). Radiation fluxes are defined as positive when directed towards the surface, and all other fluxes are defined as positive when directed away from the surface.

The available energy is equal to the observed net radiation minus soil and canopy heat fluxes. Neither soil heat flux or canopy heat flux data were available. In forests of this type soil heat flux rarely exceeds 6 W m^{-2}, approximately 1% of net radiation (Moore and Fisch, 1986). This is less than errors due to imperfect energy closure, typically 6% of net radiation. Using data from a nearby forest site, Moore and Fisch (1986) estimate that canopy heat flux can peak at ± 80 W m^{-2}, around 0800 and 2000 h in the morning and evening. This peak canopy heat flux can be a significant proportion of net radiation and it would have been desirable to include this component of the energy budget were it available.

There are a number of models of canopy conductance, from simple descriptions, such as time-of-day functions (Dolman et al., 1991), through a set of independent functions of near-surface climate (Jarvis, 1976), to models relating stomatal conductance to plant photosynthesis (Ball et al., 1987; Leuning, 1995). For the purpose of this paper the responses of canopy conductance to different meteorological forcing were to be investigated separately and for this reason a Jarvis-type model was used. Stewart (1988) established simple functional forms for several meteorological variables based on the model for leaf-level observations. These functions are usually applied at the canopy scale under the assumption that scaling is a simple function of leaf area index, L.

The general form of this model is given by the following equation:

$$g_c^{mod} = g_{max} f_1(R_s) f_2(T_1) f_3(D_1) f_4(W), \quad (2)$$

where R_s is the downward solar radiation (W m^{-2}), T_1 the reference level air temperature (°C), D_1 the reference level humidity deficit (kg kg^{-1}), and W the soil moisture (mm). The functions, f_i, take values between 0 and 1, such that in optimum conditions all the f_i are

equal to unity and canopy conductance takes the maximum value of g_{max}. Away from the optimum g_c^{mod} is reduced from g_{max} by multiplying by each f_i, some or all of which are less than unity.

Scaling from leaf to canopy level is achieved through g_{max}. Often scaling is achieved by multiplying Eq. (2) additionally by leaf area index, L, which can be constant or vary with time of year. In the absence of observations of L through the study period it was not possible to define a time varying function. However, the few measurements that have been made at primary forest sites (such as Roberts et al., 1996) indicate that there is only a small change in L of 10–15% over the course of a year. So it was assumed that L was approximately constant and could be absorbed into the optimised value of g_{max}.

Following Stewart (1988), Dolman et al. (1991) and Cox et al. (1998), the functional forms in Eq. (2) are given by

$$f_1(R_s) = \left(\frac{R_s}{1100}\right)\left(\frac{1100 + j_1}{R_s + j_1}\right), \tag{3}$$

$$f_2(T_1) = \frac{(T_1 - T_l)(T_h - T_1)^\tau}{(j_2 - T_l)(T_h - j_2)^\tau}, \tag{4}$$

$$f_3(D_1) = e^{-j_3 D_1}, \tag{5}$$

$$f_4(W) = \begin{cases} 0, & W \le \theta_w, \\ \dfrac{W - \theta_w}{\theta_c - \theta_w}, & \theta_w < W < \theta_c, \\ 1, & W \ge \theta_c, \end{cases} \tag{6}$$

where

$$\tau = \left(\frac{T_h - j_2}{j_2 - T_l}\right),$$

T_h (°C) and T_l (°C) mark the upper and lower temperature limits outside of which transpiration is assumed to cease, and j_1, j_2, j_3, θ_w and θ_c are parameters normally derived by multi-variate optimisation. The upper and lower temperatures in Eq. (4), T_h and T_l, respectively, can be included in the optimisation but are often set at values of 40 or 45 and 0 °C for the lower cut-off for the upper cut-off. There is little physiological evidence that the upper cut-off temperature is higher than 40 °C so T_h was set to this value in the optimisations.

Aerodynamic conductance, g_a, was calculated following the method of Verma (1989) with stability corrections made following Paulson (1970), as detailed in Appendix A. Roughness length, z_0, and zero plane displacement, d_0, were estimated using relationships established at another rainforest site in the same region (Shuttleworth, 1989).

As observations of soil moisture were only available at weekly intervals it was only possible to investigate the seasonal response in canopy conductance. At this time-scale, and in the absence of observations of leaf area index, it is not clear whether any change in canopy conductance is a direct or indirect response to soil moisture. The direct response would be through a decrease in leaf-level stomatal conductance for low soil moisture content, which when scaled up would give a decrease in canopy conductance. The indirect response would be that, whilst stomatal conductance does not change, leaf area index decreases as soil moisture content declines, and so the scaling factor from leaf to canopy level itself decreases.

The variable W is a measure of soil moisture, which in this case is taken as the total soil moisture content in the top 3.8 m, the depth over which observations were available. A number of other studies have used linear functions of soil matric potential, $f(\psi)$ (Shuttleworth, 1988), or non-linear functions of soil moisture deficit (Shuttleworth, 1989). A $f(W)$ function was chosen for this study as matric potential was not measured. To calculate values of ψ from the observations of W would have required a parameterisation such as van Genuchten (1980), which would have introduced a level of complexity to the optimisation not justified by the limited availability of data.

Eqs. (3)–(6) were originally proposed by Jarvis (1976), based on laboratory measurements of stomatal conductance, as empirical rather than mechanistic descriptions. They have previously been applied with success at a number of forest locations (Stewart, 1988; Wright et al., 1995).

The aim of this paper is to investigate whether a response in canopy conductance due to soil moisture is observed for an Amazonian rainforest site. This is achieved by a two-stage optimisation of the Jarvis model given by Eqs. (2)–(6). First under the assumption that there is no soil moisture dependence ($f_4 \equiv 1$ in Eq. (6)), and then by including the soil moisture function. The models were optimised by minimising the sum of square errors between modelled, g_c^{mod}, and observed, g_c^{obs}, canopy conductance.
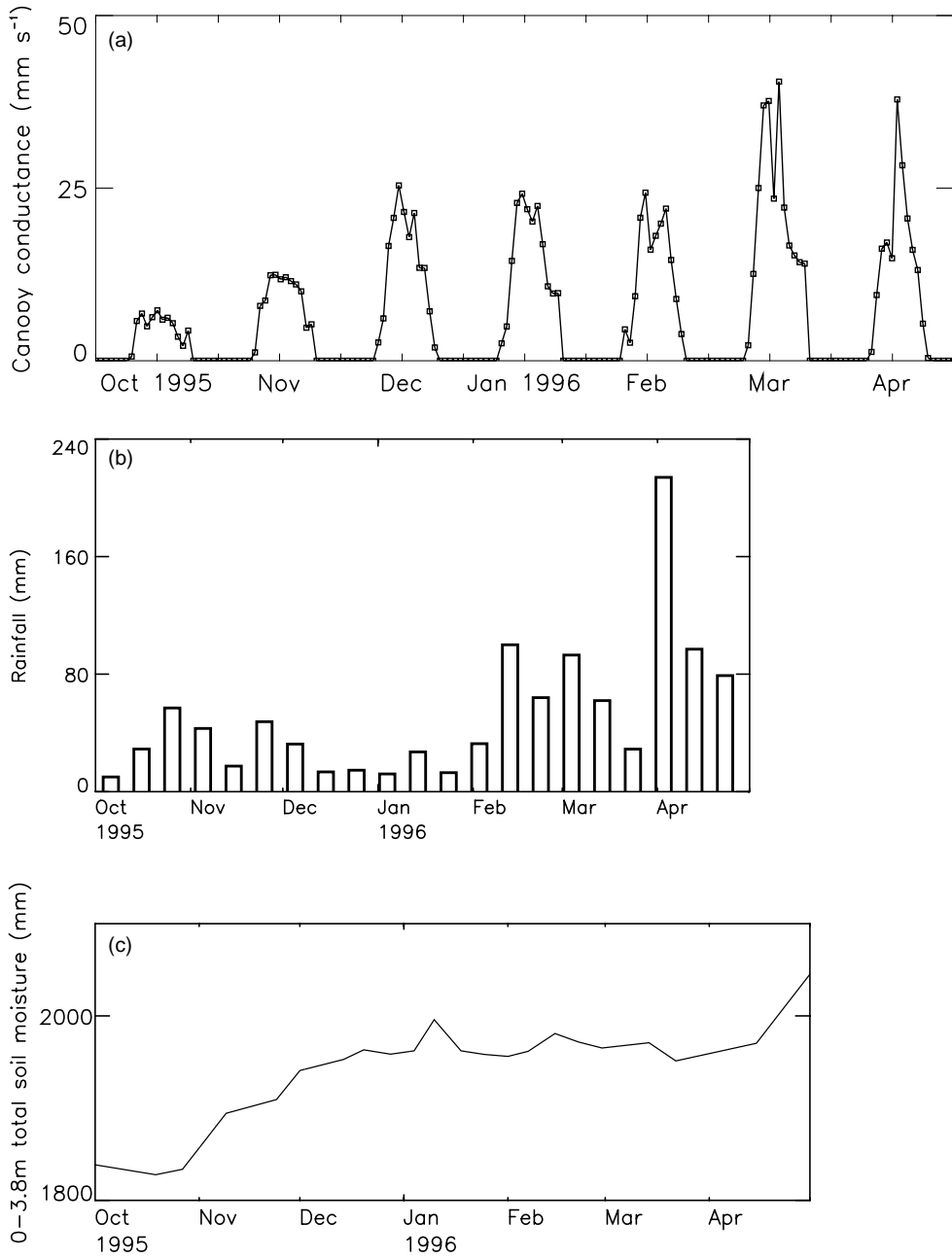
Fig. 1. Observations of: (a) mean diurnal cycles of canopy conductance for each calendar month; (b) 10-day totals of precipitation; (c) top 3.8 m total soil moisture content. In (a) data for the 634 h where canopy conductance data exist were used in the averaging. In (c) hourly values were linearly extrapolated from roughly weekly observations.

4. Results and discussion

Eddy-covariance measurements of evaporation were used in conjunction with the inverted PM equation, Eq. (1), to provide estimates of canopy conductance, g_c^{obs}. The calculated conductance values were then filtered to exclude hours when solar radiation was less than $10\,W\,m^{-2}$, as for such low incident

energy estimation of g_c^{obs} from Eq. (1) becomes overly sensitive to variation in evaporation. This typically excluded overnight hours between 1800 and 0800 h, so evening periods of canopy heat loss were excluded from the analysis, reducing errors in the calculation of available energy used in Eq. (1). The 24 h following rainfall were also excluded to avoid periods of wet-canopy evaporation. This left 634 h of canopy conductance data for optimising the model. For these remaining hours the mean and range of each of the meteorological quantities used in the Jarvis model are shown in Table 1.

Fig. 1a shows the mean diurnal cycle of canopy conductance for each calendar month of the study period. Daily maximum canopy conductance increased from October to December 1995, and this coincided with a small increase in rainfall (Fig. 1b) and a large increase in soil moisture (Fig. 1c). Between December 1995 and February 1996 there was little change in the mean diurnal cycle of canopy conductance even

Table 1
The ranges and means of the data used by the optimisation

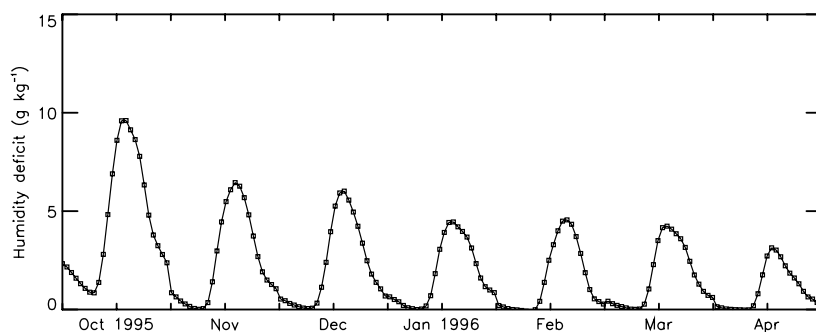|	Minimum	Maximum	Mean
Specific humidity deficit $(g\,kg^{-1})$	0.0	17.9	4.79
Air temperature (°C)	20.2	33.4	26.8
Solar radiation $(W\,m^{-2})$	11	1088	386
0–3.8 m soil moisture (mm)	1828	2015	1930
Canopy conductance $(mm\,s^{-1})$	0.0176	59.3	12.7

Fig. 2. Mean diurnal cycles of observed near-surface humidity deficit for each calendar month where observations of canopy conductance are also available.

Table 2
Parameters from optimisations of a Jarvis model of surface conductance for Amazon rainforest including, maximum canopy conductance (g_{max}), environmental functional dependencies on solar radiation (j_1), air temperature (j_2), air humidity deficit (j_3), soil moisture at wilting point (θ_w), and soil moisture at critical point (θ_c)[a]

	g_{max} $(mm\,s^{-1})$	j_1 $(W\,m^{-2})$	j_2 (°C)	j_3 $(g\,kg^{-1})$	θ_w (mm)	θ_c (mm)	Explained variance (%)
Including D_1	52.3 ± 5.2	3178 ± 1866	25.0 ± 4.5	44.2 ± 16	–	–	31.8
Including D_1 and W	52.6 ± 5.3	1785 ± 682	23.9 ± 3.6	53.9 ± 14	1766 ± 14	1961 ± 8.5	49.5
Dolman et al. (1991)	20.8	250.0	30.2	64.0	–	–	30.9
Wright et al. (1996a) including T	80.1	3916	43.1	125	–	–	35.2

[a] Column 1 indicates whether the environmental dependencies air humidity deficit (D_1), air temperature (T_1) and total 0–3.8 m soil moisture (W) were used in each model. Parameter values from previous calibrations for Amazon rainforest sites by Dolman (1993) and Wright et al. (1996a) are also included for comparison.

though rainfall decreased and then increased during this period. Soil moisture content, however, remained roughly constant through this period. Canopy conductance increased again during March and April 1996, the wettest months of the study period, when there was also a concurrent increase in soil moisture content. These changes in canopy conductance are also seen in the monthly mean diurnal cycles of humidity deficit (Fig. 2) as well as in soil moisture. Comparing Figs. 1a and 2 shows that daily maximum humidity deficit was high when daily maximum canopy conductance was low, and vice versa. Malhi et al. (2002) also examined these relationships and found that daily mean canopy conductance correlated well with soil moisture status, but the seasonal relationship with daily maximum humidity deficit was less consistent. It is this cross-correlation between soil moisture and humidity deficit that makes it difficult to assess the independent effects of them on canopy conductance.

There were either four or six parameters to be optimised in the Jarvis models depending on whether the soil moisture function was excluded or included respectively. When the soil moisture dependence was excluded the reduced Jarvis equation for canopy conductance was given by,

$$g_{c}^{mod} = g_{max} f_1(R_s) f_2(T_1) f_3(D_1).$$

Sets of optimised parameters with estimated standard errors are shown in Table 2 for Jarvis models excluding and including a soil moisture dependence. Also shown for comparison are parameter sets from Dolman et al. (1991) and Wright et al. (1996a) for other Amazonian forest sites.

Fig. 3 shows environmental response functional forms for the parameter sets in Table 2. When the soil moisture dependence was excluded the maximum canopy conductance, g_{max}, was 52.3 mm s^{-1}, comparable with the maximum observed value of 59.3 mm s^{-1} in Table 1. As g_{max} is slightly less than
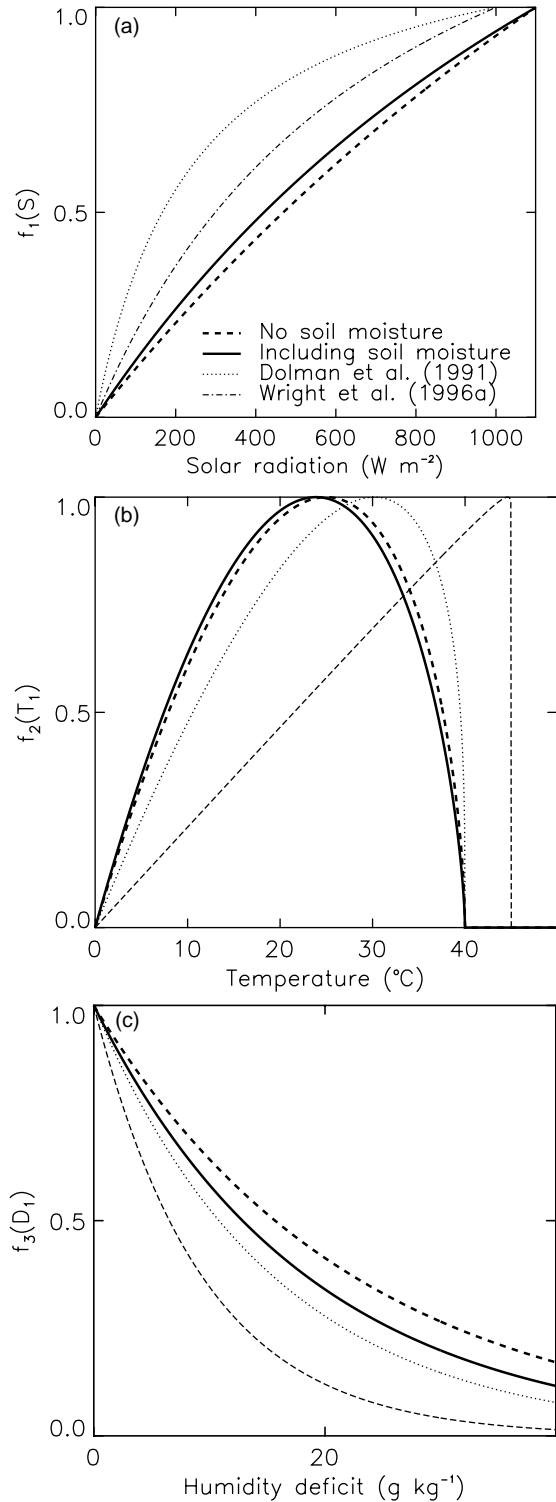

Fig. 3. Functional dependencies in the optimised Jarvis model of canopy conductance for: (a) solar radiation, R_s; (b) air temperature, T_1; (c) humidity deficit, D_1. Canopy conductance is calculated by multiplying a maximum value by the functions f_{1-3}. Functions from Dolman et al. (1991) and Wright et al. (1996b) are also shown for comparison.

the observed maximum value the model is likely to underpredict at times. The optimum temperature was 25.0 °C, which is close to the mean temperature through the observation period of 26.8 °C. The optimised solar radiation function parameter, j_1, was 3178 W m^{-2}, and for large values such as this g_c^{mod} does not saturate for high levels of solar radiation.

When the soil moisture function, f_4, was included in the optimisation the percentage of variance in the data explained by the model increased from 31.8 to 49.5%. The optimised values for θ_w and θ_c were 1766 and 1961 mm, respectively, and with low estimated standard errors compared to the estimated errors for other parameters. The parameters g_{max}, j_2 and j_3 took similar values to those when a soil moisture dependence was excluded. The solar radiation parameter, j_1, showed a large change in magnitude, but this corresponded to only a small change in the g_c^{mod} response to solar radiation (Fig. 3a). The estimated standard errors for j_1 were large for both optimisations, indicating that the model is somewhat insensitive to this parameter. Further optimisations using fixed values of j_1 showed that optimised values for the remaining parameters (j_2, j_3, θ_w, θ_c) were relatively insensitive to the choice of j_1. However, when the solar radiation response function was omitted the optimisation algorithm failed because the model was not able to describe adequately the diurnal cycle of canopy conductance from the diurnal cycles of temperature and humidity deficit.

The optimised value for θ_w of 1766 mm corresponds to an average wilting point soil moisture content over the top 3.8 m of 0.46 m^3 m^{-3}. This value is a little higher than the range 0.29–0.43 m^3 m^{-3} calculated from measurements of soil hydraulic conductivity and matric potential in similar soils to those at this site (Hodnett et al., 1996; Wright et al., 1996b), and is more comparable with observed values for critical point. The difference between the optimised critical and wilting points is 0.051 m^3 m^{-3}, which agrees with typical values of 0.045 m^3 m^{-3} observed by Ranzani (1980) for high clay content soils in Amazon rainforest. This suggests that the optimised response to changes in soil moisture is good, but the absolute values of θ_c and θ_w may be less reliable. The optimisation may have suffered from a lack of observations close to wilting point, which may have constrained θ_w closer to observed values. However, the soil moisture deficits seen in these data are still an improvement over many previous studies of canopy conductance which covered periods with no significant soil moisture stress and, therefore, were unable to provide any estimates of θ_c and θ_w.

Observations also give a typical volumetric saturated moisture content of 0.52 m^3 m^{-3} for these soils, which, along with the calibrated θ_w, would give an available water capacity of approximately 60 mm m^{-1} over the top 3.8 m. This is comparable to the relatively low values for available water content of 70 mm m^{-1} for the top 1 m and 30 mm m^{-1} for depths below 2 m quoted by Hodnett et al. (1996). Whilst the optimisation produces some physically realistic as well as functionally useful soil parameters, individual optimised parameters should only be used as part of a complete set because of the empirical nature of the model.

Optimised canopy conductance response functions for temperature yielded optimal temperatures of 25.0 and 23.9 °C. The optimal temperature quoted by Dolman et al. (1991) of 30.2 °C for a Jarvis-type model excluding a soil moisture dependence lies just outside of the error bounds estimated for these models. Sellers et al. (1997) state that the optimal temperature is close to the mean annual growing season temperature. This is supported here, as the mean air temperature for the whole data period was 25.1 °C, comparable to both optimal temperatures. The almost linear temperature response function from Wright et al. (1996a) demonstrates the problem of interdependence between parameters when optimising a Jarvis model. Over the range of temperature values used in that study (18–32 °C), the temperature function limits g_c by typically 50% to account for the relatively high optimised value of g_{max} (see Table 2). Understanding the response of canopy conductance to temperature is important for simulations of future climate change, in which many GCMs predict increased surface temperature across Amazonia.

Fig. 4 shows how including a soil moisture dependence affected the modelled monthly mean diurnal cycles of canopy conductance through the study period. When a soil moisture dependence was not included, the model overestimated peak daytime canopy conductance during a dry period between October and November. Instead the modelled peak daytime canopy conductance remained roughly constant at about 24 mm s^{-1} from October to February inclusive. When a soil moisture dependence was included the
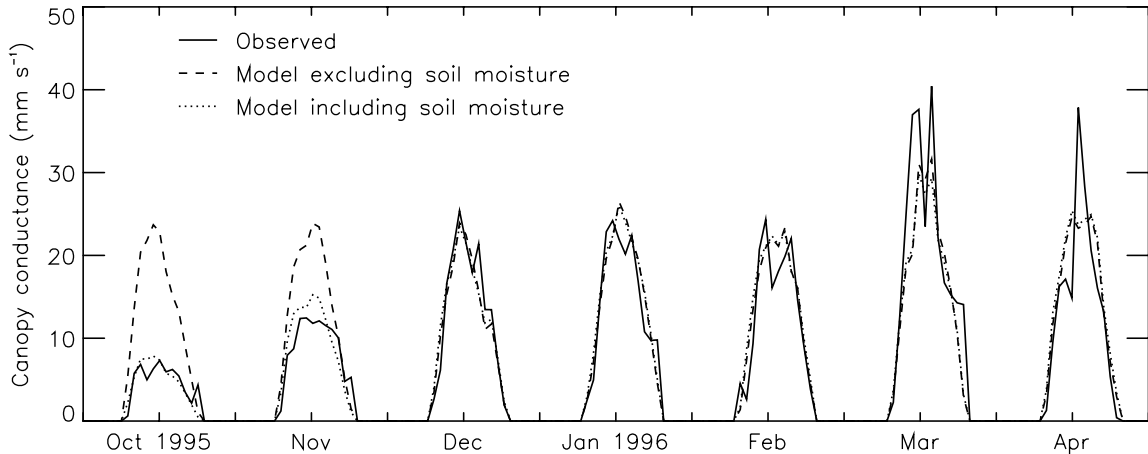
Fig. 4. Mean observed and modelled diurnal cycles of canopy conductance (g_c^{obs}) for each calendar month. Observed data used are the 634 daytime hours for rain free periods, shown by the full line. Mean diurnal cycles of canopy conductance from two models optimised excluding and including a soil moisture dependence are shown by dashed and dotted lines, respectively.

model was able to simulate the increase in canopy conductance at the beginning of the study period and, to a lesser extent, the increase during the last 2 months of the study period. The greatest change in modelled canopy conductance, when $f(W)$ was included, was seen around noon when canopy heat flux is negligible. This suggests that the effect of excluding canopy heat flux from the calculation of available energy in this study is likely to be minimal.

To analyse remaining errors in the model, hourly values of the dimensionless ratio,

$$\mu = \frac{g_c^{obs}}{g_c^{mod}}, \qquad (7)$$

were calculated, for both of the optimised models. When μ is equal to unity, the model is in exact agreement with observations; when μ is less than unity the model is overestimating canopy conductance, and vice versa. In Fig. 5a mean values of μ over 5 mm bins are plotted against soil moisture content. For the model excluding a soil moisture dependence, there is a near linear relationship between μ and W which indicates that the model tends to overpredict when soil moisture content is low. The optimised soil moisture function, also shown in Fig. 5a, follows this relationship closely, and μ values for the model including the soil moisture function are clustered around unity for low soil moistures.

A similar pattern can be seen in Fig. 5b in which μ values are plotted against humidity deficit. The model excluding a soil moisture dependence had a tendency to underpredict when humidity deficits were high, which was not present when the soil moisture function was included. The decaying form of this relationship suggested it might be possible to correct for these errors through the humidity deficit function alone. However, when the value of j_3 was adjusted so that this tendency was removed, the daily maximum modelled canopy conductance decreased through the whole of the study period rather than introducing the seasonality seen in Fig. 1a. It was only possible to achieve seasonal variation in modelled canopy conductance by including the soil moisture function, not through seasonality in the diurnal cycle of humidity deficit.

Apparent small trends can be seen in Fig. 5a and b when the soil moisture function was included, such that μ decreases with increasing soil moisture, and increases with increasing humidity deficit. This is partly a consequence of the binning, as the bins for high W and high D_1 values contain fewer data points than other bins in the range. This may also have indicated that other functional forms for $f(W)$ and $f(D_1)$ are more appropriate, although this trend was not removed when a non-linear function of W and a linear function of D_1 was used.
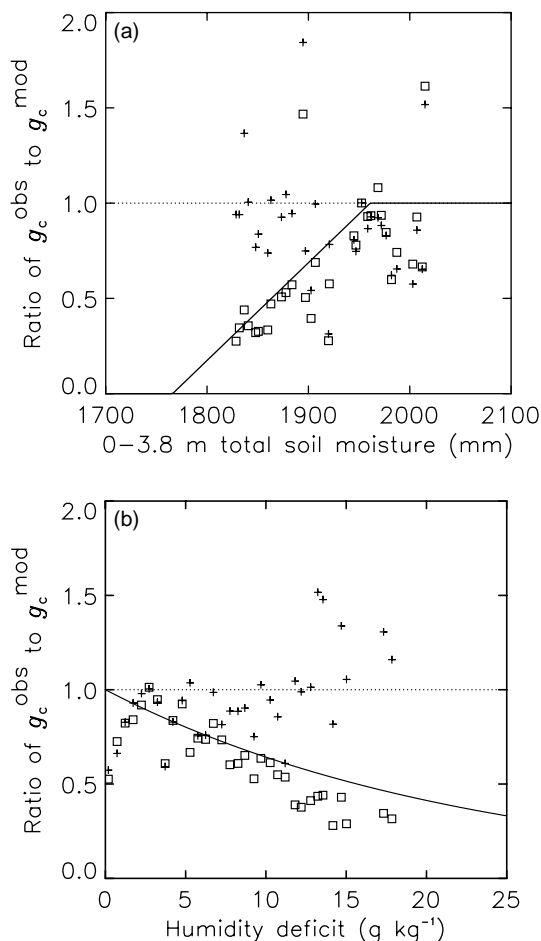
Fig. 5. Ratio of observed, g_c^{obs} to modelled, g_c^{mod} canopy conductance, μ, calculated from models that include (+) and exclude ($\square$) a soil moisture dependence plotted against: (a) 0–3.8 m total soil moisture content; (b) near-surface humidity deficit. For clarity, μ values are shown as means over 5 mm bins of soil moisture and 0.5 g kg^{-1} bins of humidity deficit. Also shown by the continuous thick lines are the optimised soil moisture function, f_4 in (a), and the optimised humidity deficit function, f_3 in (b).

This result supports the conclusions of Williams et al. (1998), who used a more complex SVAT to show that seasonal changes in soil–root hydraulic resistance could account for seasonality in evaporation. They suggest that high dry season humidity deficit would not limit evaporation if soil moisture content was high. This is confirmed here by the absence of seasonality in canopy conductance when the model excluding a soil moisture limitation was used.

As mentioned in Section 3, care must be taken when attributing this response of canopy conductance to soil moisture to either changes in leaf-level stomatal conductance or leaf area index, *L*. The inverted PM equation gives only an estimate of transpiration from the canopy as a whole, and to truly attribute the response would require observations of *L* through the study period. Nevertheless, considering that many conductance models for Amazonian rainforest neglect any soil moisture response and apply a constant value of *L*, this result is still of interest. In order to draw more detailed conclusions as to the mechanism of the response to soil moisture a more complex model is needed, such as a full SVAT scheme.

5. Summary and conclusions

In this study a Jarvis-type model of canopy conductance has been used to investigate the response of a primary forest near Manaus, Brazil, to meteorological conditions. Particular emphasis has been placed on the response to soil moisture and humidity deficit, as many previous studies neglected the former variable under an assumption that the forest had access to sufficient soil moisture to avoid water stress.

Observations of above-canopy moisture flux were used with an inverted PM equation to provide estimates of canopy conductance. Results showed that daily maximum canopy conductance increased through the study period, simultaneously with soil moisture content. However, daily maximum humidity deficit decreased through the study period, and this may also have accounted for the variation in canopy conductance.

To investigate the responses to soil moisture and humidity deficit, two Jarvis-type models of canopy conductance were optimised. Both included functions of incoming solar radiation, air temperature and humidity deficit, but one also included a function of total soil moisture in the top 3.8 m. When soil moisture was low and humidity deficit was high, the model excluding a soil moisture dependence tended to overestimate canopy conductance. As a result, there was little seasonal change in the diurnal cycle of modelled canopy conductance. Furthermore, it was not possible to correct this through the humidity deficit function, despite the observed seasonal change in this variable. When

a soil moisture dependence was included, seasonal variation in modelled canopy conductance was greatly improved. This corroborates previous studies which suggest that seasonal variation in evaporation and conductance at this site are controlled by soil moisture rather than humidity deficit. The optimised canopy conductance response functions to solar radiation, temperature and humidity deficit were similar to those when the soil moisture dependence was excluded. Uncertainty in the optimised soil moisture parameters was low, and the value for θ_w was comparable with published values calculated from measurements of soil hydraulic properties.

These results suggest that the assumption of sufficient soil moisture though all seasons is inappropriate. For this site at least, canopy conductance was limited by soil moisture as well as humidity deficit, solar radiation and temperature. While this assumption may have little effect on the simulated climate for the present day an accurate response to soil moisture is essential in simulations of future climate change in which Amazonia is significantly drier. Existing data sets of Amazonian meteorology and moisture flux may not display sufficient seasonality and inter-annual variability for all stomatal responses to be established. Data sets covering periods of several years, including El Niño cycles, are needed to improve the modelled land-surface response for situations significantly different from current climate.

Acknowledgements

Appendix A

Aerodynamic conductance, g_a, is calculated as

$$\frac{1}{g_a} = \left[\frac{u}{u_*^2} + \frac{1}{ku_*} \left(\ln\left(\frac{z_0}{z_{0t}}\right) + \Psi_M - \Psi_H \right) \right], \quad (A.1)$$

in which u is the near-surface wind speed ($m\,s^{-1}$), u_* the friction velocity ($m\,s^{-1}$), k the von Karman

Table 3
Values of reference height (z_r), roughness length (z_0), displacement height (d) and the ratio d/h, where h is the canopy height, used in the calculation of aerodynamic resistance for a tropical forest site[a]

Length scale	Value here	Shuttleworth (1988)	Dolman (1993)	Gash et al. (1996)
z_r (m)	46	45	–	35.0
z_0 (m)	1.8	3.5	1.0	2.1
d (m)	25.8	26.3	23	30.1
d/h	0.86	0.75	0.66	0.86

[a] Values from literature are shown for comparison.

constant (0.41), z_0 and z_{0t} are the roughness lengths for heat and momentum, respectively (m), and Ψ_H and Ψ_M are the stability correction terms for heat and momentum, respectively. The roughness length for momentum, z_{0t}, is calculated as $z_0\,e^{-2}$.

An initial estimate of u_* is made using

$$u_* = \frac{ku}{\ln((z_r - d)/z_0)}, \quad (A.2)$$

where z_r is the reference height at which observations were taken (m), d the displacement height (m), and z_0 the roughness length (m). Values for these length scales are given in Table 3 along with other values from the literature for comparison. The displacement height, d, and roughness length, z_0, are assumed to be 0.86 and 0.06 of the canopy height, respectively, following Shuttleworth (1989).

The initial estimate of u_* allows calculation of the Monin–Obukov length, m_0, and ζ using,

$$m_0 = \frac{-\rho c_p u_*^3 T_d}{kg(H + 0.07\lambda E)}, \quad (A.3)$$

$$\zeta = \frac{z_r - d}{m_0}, \quad (A.4)$$

ζ is then used to calculate the corrections using Eqs. (A.5) and (A.6), following Paulson (1970):

$$\Psi_M = \begin{cases} 2\ln(\frac{1}{2}(1 + \zeta_0)) + \ln(\frac{1}{2}(1 + \zeta_0^2)) \\ \quad -2\arctan(\zeta_0) + 1.5708, & \zeta \leq 0, \\ \quad\quad\quad -5\zeta_0, & \zeta > 0, \end{cases} \quad (A.5)$$

$$\Psi_H = \begin{cases} 2\ln(\frac{1}{2}(1 + \zeta_0^2)), & \zeta \leq 0, \\ \quad -5\zeta_0, & \zeta > 0, \end{cases} \quad (A.6)$$

where

$$\zeta_0 = (1 - 16\zeta)^{1/4}. \tag{A.7}$$

These allow the calculation of a corrected u_* using

$$u_* = \frac{ku}{\ln((z_r - d)/z_0) - \Psi_M}. \tag{A.8}$$

References

Ashby, M., 1999. Modelling the water and energy balances of Amazonian rainforest and pasture using Anglo-Brazilian Amazonian climate observation study. Agric. For. Meteorol. 94, 79–101.

Ball, J., Woodrow, I., Berry, J., 1987. A model predicting stomatal conductance and its contribution to the control of photosynthesis under different environmental conditions. In: Biggins, I. (Ed.), Progress in Photosynthesis Research. Martinus Nijhoff, The Netherlands, pp. 221–224.

Correa, J., 1984. Características físico hídricas dos solos latossolo amarelo, podzolico vermelho amarelo e podzol hidromórfico do estado do Amazonas. Pesquisa Agropecuaria Brasileira 20, 1317–1322.

Costa, M., Foley, J., 1999. Trends in the hydrologic cycle of the Amazon basin. J. Geophys. Res. 104 (D12), 14189–14198.

Cox, P., Huntingford, C., Harding, R., 1998. A canopy conductance and photosynthesis model for use in a GCM land surface model. J. Hydrol. 212-213, 79–94.

Cox, P., Betts, R., Jones, C., Spall, S., Totterdell, I., 2000. Acceleration of global warming due to carbon-cycle feedbacks in a coupled climate model. Nature 408, 184–187.

Dolman, A., 1993. A multiple-source land surface energy balance model for use in general circulation models. Agric. For. Meteorol. 65, 21–45.

Dolman, A., Gash, J., Roberts, J., Shuttleworth, W., 1991. Stomatal and surface conductance of tropical rainforest. Agric. For. Meteorol. 54, 303–318.

Gash, J., Nobre, C., Roberts, J., Victoria, R. (Eds.), 1996. Amazonian Deforestation and Climate. Wiley, Chichester, UK.

Hahmann, A., Dickinson, R., 1997. RCCM2-BATS model over tropical South America: applications to tropical deforestation. J. Clim. 10 (8), 1944–1964.

Hastenrath, S., 1997. Annual cycle of upper air circulation and convective activity over the tropical Americas. J. Geophys. Res. 102, 4267–4274.

Hodnett, M., Tomasella, J., Marques Filho, O., Oyama, M., 1996. Deep soil water uptake by forest and pasture in central Amazonia: predictions from long term daily rainfall data using a simple water balance model. In: Gash, J., Nobre, C., Roberts, J., Victoria, R. (Eds.), Amazonian Deforestation and Climate. Wiley, Chichester, UK, Chapter 4, pp. 79–100.

Jarvis, P., 1976. The interpretation of the variations in leafwater potentials and stomatal conductances found in canopies in the field. Philos. Trans. R. Soc. London Ser. B 273, 593–610.

Leuning, R., 1995. A critical appraisal of a combined stomatal-photosynthesis model for C_3 plants. Plant Cell Environ. 18, 357–364.

Malhi, Y., Nobre, A., Grace, J., Kruijt, B., Pereira, M., Culf, A., Scott, S., 1998. Carbon dioxide transfer over a Central Amazonian rainforest. J. Geophys. Res. 103 (D24), 31593–31612.

Malhi, Y., Pegoraro, E., Nobre, A., Pereira, M., Grace, J., Culf, A., Clement, R., 2002. Energy and water dynamics of a central Amazonian rain forest. J. Geophys. Res. 107 (D20), 8061.

Monteith, J., 1981. Evaporation and surface temperature. Quart. J. R. Meteorol. Soc. 107, 1–27.

Moore, C., Fisch, G., 1986. Estimating heat storage in Amazonian tropical forest. Agric. For. Meteorol. 38, 245–269.

Nepstad, D., de Carvalho, C., Davidson, E., Jipp, P., Lefebvre, P., Negreiros, G., da Silva, E., Stone, T., Trumbore, S., Vieira, S., 1994. The role of deep roots in the hydrological and carbon cycles of Amazonian forests and pastures. Nature 372, 666–669.

Nobre, C., Sellers, P., Shukla, J., 1991. Amazonian deforestation and regional climate change. J. Clim. 4 (10), 957–988.

Paulson, C., 1970. The mathematical representation of wind speed and temperature profiles in the unstable atmospheric surface layer. J. Appl. Meteorol. 9, 857–861.

Ranzani, G., 1980. Indentificação e caracterização de alguns solos da Estação Experimental de Silvicultura Tropical do INPA. Acta Amazonica 10, 7–41.

Roberts, J., Cabral, O., da Costa, J., McWilliam, A.-L., 1996. An overview of the leaf area index and physiological measurements during ABRACOS. In: Gash, J., Nobre, C., Roberts, J., Victoria, R. (Eds.), Amazonian Deforestation and Climate. Wiley, Chichester, UK, Chapter 16, pp. 287–306.

Sellers, P., Dickinson, R., Randall, D., Betts, A., Hall, F., Berry, J., Collatz, G., Denning, A., Mooney, H., Nobre, C., Sato, N., Field, C., Henderson-Sellers, A., 1997. Modelling the exchanges of energy, water, and carbon between continents and the atmosphere. Science 275, 502–509.

Shuttleworth, W., 1988. Evaporation from Amazonian rainforest. Proc. R. Soc. London Ser. B 233, 321–346.

Shuttleworth, W., 1989. Micrometeorology of temperate and tropical forest. Philos. Trans. R. Soc. London Ser. B 324, 299–334.

Sommer, R., Sá, T.d.A., Vielhauer, K., de Araújo, A., Fölster, H., Vlek, P., 2002. Transpiration and canopy conductance of secondary vegetation in the eastern Amazon. Agric. For. Meteorol. 112, 103–121.

Stewart, J.B., 1988. Modelling surface conductance of pine forest. Agric. For. Meteorol. 43, 19–35.

Stocker, T., Clarke, G., Le Treut, H., Lindzen, R., Meleshko, V., Mugara, R., Palmer, T., Pierrehumbert, R., Sellers, P., Trenberth, K., Willebrand, J., 2001. Physical climate processes and feedbacks. In: Houghton, J., Ding, Y., Griggs, D., Hoguer, M., van der Linder, P., Dai, X., Maskell, K., Johnson, C. (Eds.), Climate Change 2001: The Scientific Basis. Contribution of Working Group I to the Third Assessment Report of

the Intergovernmental Panel on Climate Change. Cambridge University Press, Cambridge, Chapter 7, pp. 419–470.

van Genuchten, M., 1980. A closed-form equation for predicting the hydraulic conductivity of unsaturated soils. Soil Sci. Soc. Am. J. 44, 892–898.

Verma, S., 1989. Aerodynamic resistances to transfers of heat, mass and momentum in estimation of areal evaporation. IAHS Publ., p. 177.

White, A., Cannell, M., Friend, A., 1999. Climate change impacts on ecosystems and the terrestrial carbon sink: a new assessment. Glob. Environ. Change 9, S21–S30.

Williams, M., Malhi, Y., Nobre, A., Rastetter, E., Grace, J., Pereira, M., 1998. Seasonal variation in net carbon exchange and evapotranspiration in a Brazilian rain forest: a modelling analysis. Plant Cell Environ. 21, 953–968.

Wright, I., Manzi, A., da Rocha, H., 1995. Surface conductance of Amazonian pasture: model application and calibration for canopy climate. Agric. For. Meteorol. 75, 51–70.

Wright, I., Gash, J., da Rocha, H., Roberts, J., 1996a. Modelling surface conductance for Amazonian pasture and forest. In: Gash, J., Nobre, C., Roberts, J., Victoria, R. (Eds.), Amazonian Deforestation and Climate. Wiley, Chichester, UK, Chapter 26, pp. 437–458.

Wright, I., Nobre, C., da Rocha, H., Roberts, J., Vertamatti, E., Culf, A., Santos-Alvala, R., Hodnett, M., Ubarana, V., 1996b. Towards a GCM parameterization for Amazonia. In: Gash, J., Nobre, C., Roberts, J., Victoria, R. (Eds.), Amazonian Deforestation and Climate. Wiley, Chichester, UK, Chapter 28, pp. 473–504.